Organic & Biomolecular Chemistry

PAPER

View Article Online
View Journal | View Issue

Cite this: *Org. Biomol. Chem.*, 2019, **17**, 8918

Deeper insight into protease-sensitive "covalent-assembly" fluorescent probes for practical biosensing applications†‡

Kévin Renault, [a] Sylvain Debieu,§[a] Jean-Alexandre Richard [b] and Anthony Romieu *[a]

Received 12th August 2019,
Accepted 19th September 2019

DOI: 10.1039/c9ob01773a

rsc.li/obc

We report a rational and systematic study devoted to the structural optimisation of a novel class of protease-sensitive fluorescent probes that we recently reported (S. Debieu and A. Romieu, *Org. Biomol. Chem.*, 2017, **15**, 2575–2584), based on the "covalent-assembly" strategy and using the targeted enzyme penicillin G acylase as a model protease to build a fluorescent pyronin dye by triggering a biocompatible domino cyclisation–aromatisation reaction. The aim is to identify *ad hoc* probe candidate(s) that might combine fast/reliable fluorogenic "turn-on" response, full stability in complex biological media and ability to release a second molecule of interest (drug or second fluorescent reporter), for applications in disease diagnosis and therapy. We base our strategy on screening a set of active methylene compounds (C-nucleophiles) to convert the parent probe to various pyronin caged precursors bearing Michael acceptor moieties of differing reactivities. *In vitro* stability and fluorescent enzymatic assays combined with HPLC-fluorescence analyses provide data useful for defining the most appropriate structural features for these fluorogenic scaffolds depending on the specifications inherent to biological application (from biosensing to theranostics) for which they will be used.

Introduction

In the growing field of small molecule activatable (or "smart") fluorescent probes for biological and environmental analysis and bioimaging (*i.e.*, biomedical applications related to *in vivo* molecular imaging, image-guided drug delivery and theranostics), innovation is a primary concern as evidenced by numerous valuable research studies published annually.[1] It focuses mainly on both the development of high performance organic-based fluorophores[2] and discovery of novel and effective approaches/mechanisms to optimize the fluorogenic response (intensometric or ratiometric detection mode) arising from selective interaction/reaction of the probe with its supposed target (bio)analyte.[3] The ultimate goal is to improve detection sensitivity regardless of the complexity of the biological/environmental matrices to be analysed.

By the mid 2000s, a new probe design principle namely the "covalent-assembly" approach had emerged as a valuable alternative to conventional pro-fluorophores based on the protection–deprotection of an optically tunable amino or hydroxyl group.[4] Originally proposed by Anslyn and Yang,[5] the basic rationale of the "covalent-assembly" type probes is the formation of a fluorophore *via* a covalent cascade reaction of two fragments that most commonly proceeds in an intramolecular manner and is triggered by the species to be detected. The fundamental feature of the "covalent-assembly" probe is that it guarantees both a colorimetric change (except for UV-absorbing fluorophores such as traditional 7-*N*,*N*-dialkylamino or 7-hydroxycoumarins) and an optimal "turn-on" fluorescent signal from a zero background.[6] Alternatively, the "covalent-assembly" process occurring from an "already-on" fluorescent caged precursor may sometimes lead to a new electronic push–pull conjugated backbone and thus causes a significant "red-shift" of the fluorescence spectra particularly well-suited for devising ratiometric detection schemes.[7] The vast majority of "covalent-assembly" type probes already published, more than

[a]*ICMUB, UMR 6302, CNRS, Univ. Bourgogne Franche-Comté, 9, Avenue Alain Savary, 21000 Dijon, France. E-mail: anthony.romieu@u-bourgogne.fr; http://www.icmub.com*

[b]*Functional Molecules and Polymers, Institute of Chemical and Engineering Sciences (ICES), Agency for Science, Technology and Research (A*STAR), 8 Biomedical Grove, Neuros, #07–01, Singapore 138665. E-mail: jean_alexandre@ices.a-star.edu.sg*

†A preprint was previously posted on ChemRxiv, see https://doi.org/10.26434/chemrxiv.9445202.v1

‡Electronic supplementary information (ESI) available: Experimental details related to photophysical characterisation, fluorescence-based *in vitro* assays and HPLC-fluorescence/-MS analyses and all analytical data of the synthesised compounds. See DOI: 10.1039/c9ob01773a

§Present address: PSL Université Paris, Institut Curie, CNRS UMR 3666, INSERM U1143, 75005 Paris France.

60 examples dealing with the detection of a wide range of analytes including biothiols, enzymes, metal cations and ROS/RNS, involve *in situ* formation of blue-green emitting 7-*N*,*N*-dialkylamino/7-hydroxy-(2-imino)coumarins or related fluorophores through analyte-triggered lactonisation or Pinner cyclisation reactions.[5a,8] To expand this innovative molecular sensing approach to longer-wavelength fluorophores, we along with the Yang group have recently designed "covalent-assembly" type probes whose activation leads to the internal construction of xanthene dyes emitting in the range 550–625 nm. This is a major achievement supported by *in vitro* fluorogenic detection assays of relevant analytes including: Sarin mimics and Hg(II) cations (*in situ* formation of pyronin B),[9] proteases namely penicillin G acylase (PGA) and leucine amino peptidase (LAP) (*in situ* formation of unsymmetrical pyronin **AR116**, Fig. 1)[10] and nitrogen dioxide $NO_2^{\bullet}$ (*in situ* formation of a rosa-

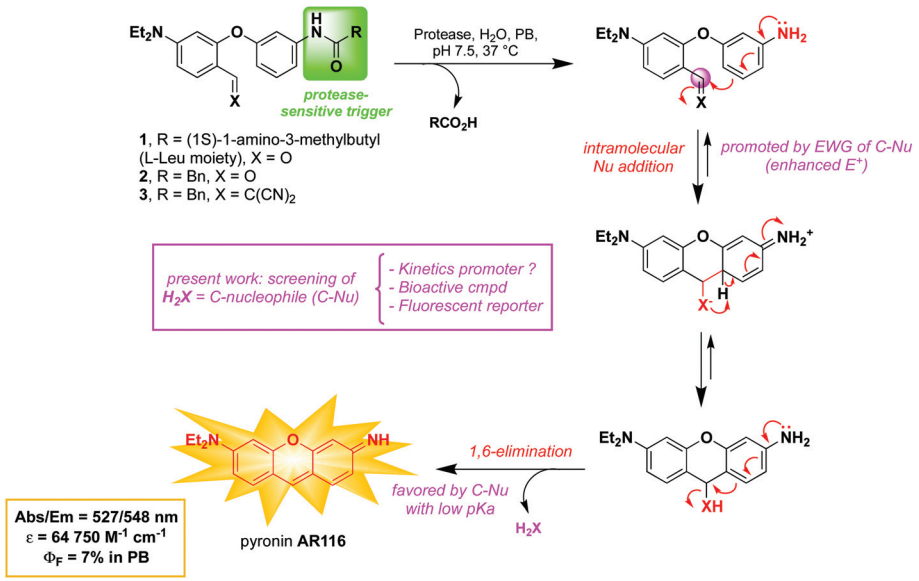

Fig. 1 State-of-the-art (structures and detection mechanism) "covalent-assembly" type probes for protease sensing through *in situ* formation of unsymmetrical pyronin **AR116**. In magenta colour, the approach chosen in the present work for the rational optimisation of these probes, to find the best compromise between reactivity, stability and versatility with the possible concomitant release of a second molecule of interest (Bn = benzyl, EWG = electron-withdrawing group, PB = phosphate buffer).

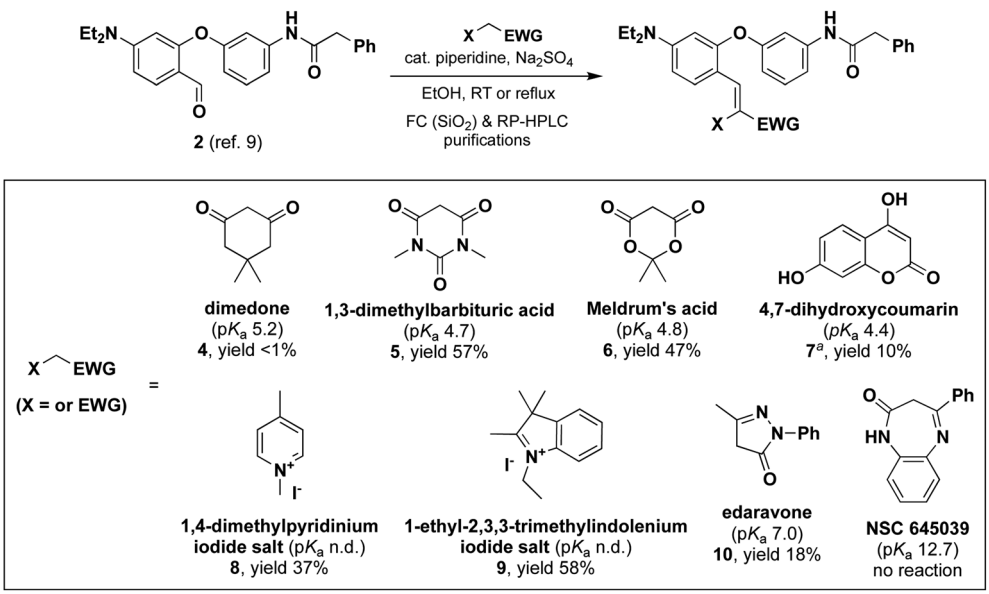

Scheme 1 Synthesis of Michael acceptor-based PGA-sensitive probes **4–10** through the Knoevenagel condensation reaction. [a]For the structure of probe **7**, see Fig. 5. Please note: probes **7–9** were isolated as TFA salts (EWG = electron-withdrawing group, FC (SiO_2) = flash-column chromatography over silica gel, RT = room temperature). Please note: molecule numbering **4–10** corresponds to probe's description and not C-nucleophiles used for their preparation.

mine).[11] These encouraging results have convinced us that the "covalent-assembly" approach may have great potential to facilitate (1) the design of "smart" *in vivo* imaging agents (activated by disease-associated enzymes)[12] and (2) their possible conversion to fluorogenic reaction-based prodrug conjugates (*i.e.*, theranostic agents)[13] for diagnostic and therapeutic purposes. However, to achieve these ambitious goals, first of all it is essential to demonstrate that enzyme-triggered xanthene formation is a versatile process, not negatively impacted by interferences found in biological media (*e.g.*, biothiols). Equally important will be the demonstration that kinetics can be easily fine-tuned and the cascade mechanism can be readily applied to the concomitant release of bioactive compounds. This will entail significant efforts geared toward the structural optimization of caged precursors based on a mixed bis-aryl ether core structure[10] (Fig. 1). To rapidly reach a representative range of such "covalent-assembly" type probes, the conversion of the formyl group (found in probes **1** and **2**) to various Michael acceptor moieties through Knoevenagel condensation may well be the preferred route (Scheme 1). Indeed, numerous latent C-nucleophiles are stable, cheap and commercially available and their structural diversity (related to their pK_a value) offers a unique opportunity for adjusting the subtle balance between the stability and reactivity of the probes under aqueous physiological conditions. Furthermore, such reactive moieties may be found in molecules either displaying a specific biological activity (*e.g.*, benzodiazepinone and 5-pyrazolone derivatives) and/or acting as a second fluorescent reporter (*e.g.*, 4,7-dihydroxycoumarin).

Herein, we report the synthesis of eight different PGA-sensitive "covalent-assembly" fluorogenic probes whose Michael acceptor moiety stems from parent C-nucleophiles covering a broad range of pK_a values (from 4.4 to 12.7). Their fluorogenic behavior as well as their enzymatic activation and aqueous stability were studied in detail through *in vitro* fluorescence assays and HPLC-fluorescence/-MS analyses. All data generated have been used to establish which Michael acceptors are suited to serve in the design of caged precursors of fluorescent unsymmetrical pyronins, depending on the specifications required by the targeted fluorescence-based bioanalysis or bioimaging application.

Results and discussion

As briefly reminded above, our group has recently shown that proteases (*i.e.*, PGA and LAP) are able to build the xanthene-based fluorophore **AR116** from mixed bis-aryl ether caged precursors (probes **1** and **2**) and through a biocompatible cyclisation/aromatisation process triggered by this biological stimulus.[10] However, the kinetics of pyronin formation was too slow (over 10 h to achieve a significant level of fluorescence) for considering the implementation of such "covalent-assembly" type probes in diagnostic bioassays or in the most challenging context of *in vivo* fluorogenic imaging of disease-relevant enzymes. A considerable increase in the rate of *in situ* pyronin formation was achieved by converting the formyl group of **2** into the dicyanomethylidenyl moiety (less than 1 h to achieve quantitative formation of **AR116**).[14] However, the resulting PGA-sensitive probe **3** acts as a fluorogen with aggregation-induced emission (AIEgen)[15] displaying an intense red fluorescence (emission centered at *ca.* 600 nm with a quantum yield of 6%) that prevents detection according to an intensometric approach. Furthermore, its aqueous stability and possible undesired reactivity with molecules currently found in biological media have not yet been carefully studied. To address these items and to identify the best protease-triggered reaction-based probe candidates that might combine fast/reliable fluorogenic "turn-on" response, overall stability and ability to release a second molecule of interest (in addition to pyronin **AR116**), we have screened a short library of C-nucleophiles whose reaction with aldehyde **2** should lead to a set of probes exhibiting their own intrinsic reactivity closely tied to the pK_a value of the nucleophilic partner involved in their synthesis. To cover a broad range of C-nucleophiles that fulfills the requirements mentioned above, we have chosen to use both commercial basic organic building blocks and less conventional molecular structures: dimedone (pK_a 5.2 in water),[16] 1,3-dimethylbarbituric acid (pK_a 4.7 water),[17] Meldrum's acid (pK_a 4.8 in water),[16,18] 4,7-dihydroxycoumarin (pK_a 4.4 in water, see the ESI‡ for its photophysical characterization in phosphate buffer (PB)),[19] 1,4-dimethylpyridinium iodide (pK_a never determined), 1-ethyl-2,3,3-trimethylindolenium iodide (pK_a never determined), edaravone (a free radical scavenger and neuroprotective agent used for the therapy of amyotrophic lateral sclerosis, also known as 1-phenyl-3-methyl-5-pyrazolone, pK_a 7.0 in water)[20] and NSC 645039 (4-phenyl-1,3-dihydro-2*H*-1,5-benzodiazepin-2-one, pK_a 12.7, predicted value),[21] compared with malononitrile (pK_a 11.5).[22]

Synthesis of Michael acceptor-based caged precursors through Knoevenagel condensation

The one-step synthesis of Michael acceptors **4–10** was achieved from the known benzaldehyde derivative **2** and the corresponding C-nucleophile, using conditions previously optimised for the preparation of dicyanomethylidene-based probe **3** (*i.e.*, cat. piperidine, anhydrous Na_2SO_4, EtOH).[14] When this condensation reaction was performed at room temperature, the formation of the desired product was only observed with dimedone, 1,3-dimethylbarbituric acid and Meldrum's acid as C-nucleophiles. It is important to note that the reaction with dimedone is less efficient with many side-products being formed due to the great electrophilic reactivity of the resulting dimedone-based Michael acceptor **4**. Heating under reflux was effective to provide the condensation adducts derived from less usual C-nucleophiles. However, under these latter conditions, 4-phenyl-1,3-dihydro-2*H*-1,5-benzodiazepin-2-one was found to be unreactive toward benzaldehyde **2** and we failed to obtain the claimed caged precursor. Alternative conditions (*i.e.*, the use of NaOAc as a base in AcOH under reflux) previously reported for the Knoevenagel

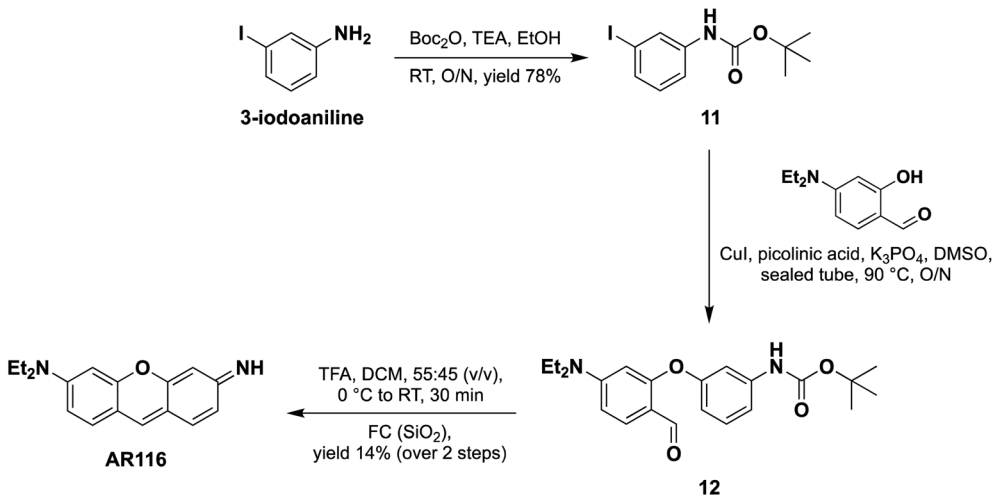

Scheme 2 Optimised synthesis of unsymmetrical pyronin **AR116**. (Boc_2O = di-*tert*-butyl dicarbonate, FC (SiO_2) = flash-column chromatography over silica gel, O/N = overnight, RT = room temperature).

condensation between NSC 645039 and 4-(dimethylamino) benzaldehyde[23] were also tested but degradation of benzaldehyde **2** and its cyclisation into the *N*-phenylacetyl derivative of pyronin **AR116** were observed. All PGA-sensitive "covalent-assembly" fluorogenic probes were isolated in moderate to good yields (except for dimedone adduct **4**) by conventional flash-chromatography on silica gel. Optimal purity (>95%) required for fluorescence measurements and enzymatic assays was readily achieved by further purification by semi-preparative RP-HPLC. Since compounds **4–6** and **10** were found to be poorly stable under aqueous acidic conditions (*i.e.*, 0.1% aqueous formic acid and trifluoroacetic acid), ultrapure water and MeCN were used as eluents. Conversely, 4,7-dihydroxycoumarin adduct **7** and hemicyanine-like derivatives **8** and **9** are fully stable under aqueous acidic conditions and were recovered as TFA salts. The mass percentages of TFA (17%, 16.5% and 19% respectively, corresponding to *ca.* one molecule of TFA per molecule of probe) in freeze-dried samples were determined by ionic chromatography. All spectroscopic data (see ESI‡), especially IR, NMR and mass spectrometry, were in agreement with the structures assigned. Their purity was checked by RP-HPLC and found to be above 95% with the exception of Knoevenagel adducts poorly stable under aqueous acidic conditions (see ESI‡). Surprisingly, the Michael acceptor moiety of the 4,7-dihydroxycoumarin adduct is sufficiently electrophilic to undergo an intramolecular nucleophilic addition of the adjacent phenylogous *N*-phenylacetylamine unit yielding unprecedented *N*-acyl rosamine dye **7** based on a pyronin–coumarin hybrid skeleton (Fig. 5). In addition to these syntheses, we have also re-examined the preparation of unsymmetrical pyronin **AR116** (used as a reference for *in vitro* fluorescence assays and HPLC-fluorescence analyses) with the aim of both improving the isolated yield and facilitating its purification. Indeed, Brønsted acid-mediated condensation of 4-(diethylamino)salicylaldehyde with 3-aminophenol did not work well and the isolation of **AR116** from the crude mixture required three successive purifications on C_{18}-reversed phase silica (very poor isolated yield <2%).[10] In addition, the recovered fluorophore was still contaminated with a minor amount (less than 10%) of the starting aldehyde. To circumvent these difficulties, a two-step synthetic route based on (1) Ullman-type coupling between *N*-Boc-3-iodoaniline **11** and 4-(diethylamino)salicylaldehyde and subsequent (2) TFA-mediated cascade deprotection–cyclisation–dehydration reaction was devised (Scheme 2). As expected, the purification of **AR116** was greatly facilitated and the isolated yield was dramatically improved (14% over two steps).

Comparative enzymatic activation of Michael acceptor-based caged precursors

Before launching the campaign of fluorescence-based *in vitro* assays with commercial PGA enzymes (from *Escherichia coli*), we have studied the photophysical properties of probes **4–10** in phosphate buffer (100 mM, pH 7.6) containing less than 1% of DMSO originating from the dilution of 1.0 mg mL^{-1} stock solution in this latter solvent (see Fig. S1–S7‡ for the corresponding spectral curves). All PGA-sensitive probes **4–10** exhibit a strong electronic absorption either in the blue-cyan region (Abs λ_{max} centered around 470–495 nm with ε in the range 32 300–29 500 M^{-1} cm^{-1} for probes **4–6**, **8** and **10**) or in the green-yellow spectral range for *N*-phenylacetyl rosamine **7** (Abs λ_{max} = 507 and 552 nm, ε = 36 900 and 34 800 M^{-1} cm^{-1}) and hemicyanine-like derivative **9** (Abs λ_{max} = 548 nm, ε = 67 900 M^{-1} cm^{-1}) that contain a more extended conjugated π system. Unlike the malononitrile adduct **3**, the excitation of these probes did not produce detectable light emission (except for Meldrum's acid adduct **6** and hemicyanine-like derivative **9**, with weak emission centered at 612 and 593 nm respectively and poor quantum yield determined at 1% or less, see the ESI‡ for detailed information) and the aggregation-induced emission (AIE) phenomenon was not observed. The main consequence of this zero-background fluorescence for these caged

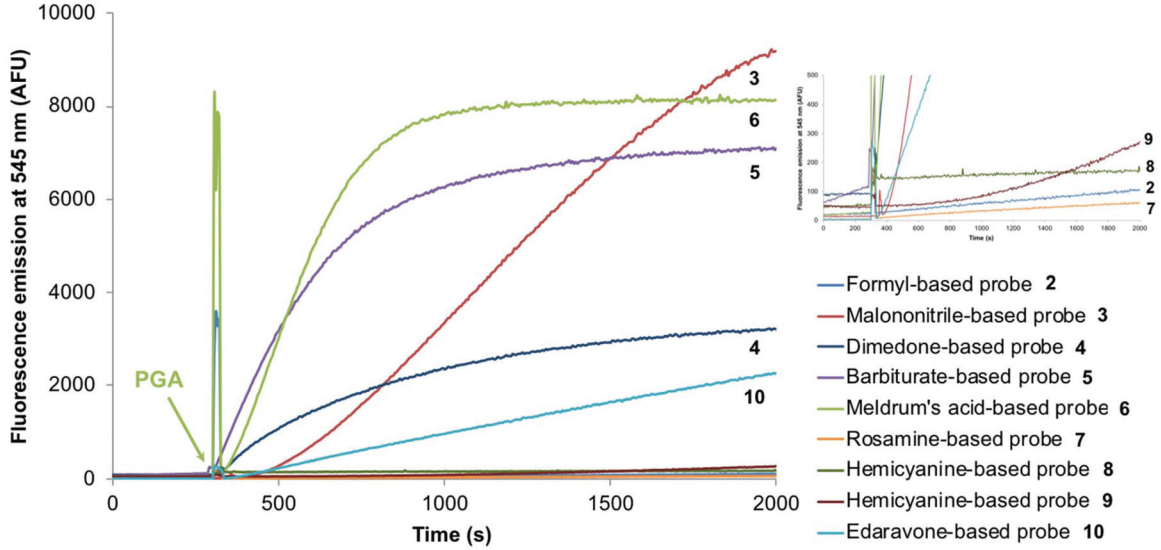

Fig. 2 Time-dependent changes in the green-yellow fluorescence intensity (Ex./Em. 525/545 nm, slit 5 nm) of fluorogenic probes **2–10** (concentration: 1.0 μM) in the presence of PGA (1 U) in PB (100 mM, pH 7.6) at 37 °C. Please note: PGA was added after 5 min of incubation of probe in PB alone.

precursors is that the detection of PGA enzyme activity can be achieved through an intensometric fluorogenic response.

All fluorogenic PGA assays and blank experiments were achieved through time-course measurements following a reliable protocol previously developed by us. The resulting kinetic curves are shown in Fig. 2 (see Fig. S10–S16‡ for blank curves). Since the quantitative conversion of the reference probe (*i.e.*, dicyanomethylidene-based probe **3**) into pyronin **AR116** occurs within 30 min, this duration was chosen for all kinetics. A rapid and gradual increase of fluorescence emission at 545 nm (Ex. 525 nm) was observed with three PGA-sensitive Michael acceptor-based caged precursors **4–6**. These results are consistent with both our expectations and low pK_a values of C-nucleophiles (acting as the best leaving groups) released through the 1,6-elimination process leading to xanthene aromatisation (*i.e.*, dimedone, 1,3-dimethylbarbituric acid and Meldrum's acid). However, the level of fluorescence achieved is somewhat lower than that of the reference probe **3**, particularly for the dimedone adduct (3200 AFU *vs.* 9200 AFU within 30 min) suggesting poor aqueous stability at physiological temperature of this "covalent-assembly" type probe. Indeed, the nucleophilic addition of a water molecule (or hydroxide ion) to its activated double bond should lead to the release of dimedone and unveiling of the aldehyde functional group through a retro-Knoevenagel process. The propensity of probes **5** and **6** to undergo such undesired hydrolysis is much more limited and this feature was further supported by comprehensive stability studies (*vide infra*). Interestingly, a slower but still gradual increase of green-yellow fluorescence intensity was obtained with the pyrazolone adduct **10** (2270 AFU within 30 min). This decrease of the kinetics of pyronin formation is closely related to both the (1) higher pK_a value of edaravone that may be regarded as a less good leaving group than dimedone, 1,3-dimethylbarbituric acid and Meldrum's acid and (2) lower electrophilicity of the Michael acceptor compared to that of the dicyanomethylidenyl moiety. Thus, the rate of the tandem cyclisation–aromatisation process is negatively impacted. The positive counterpart of the relative lack of reactivity of this probe is its full aqueous stability that is a key parameter of theranostic agents. The presence of free edaravone in the enzymatic reaction mixture was unambiguously confirmed by HPLC-MS analysis carried out after a prolonged time of incubation (20 h, see Fig. 3 and Fig. S38–S41‡). This product was identified through its HPLC retention time (t_R = 2.6 min, MS(ESI+): m/z = 175.5 $[M + H]^+$, calcd for $C_{10}H_{11}N_2O^+$ 175.1) comparison and co-injection with commercial reference but also by MS analysis (full-scan and SIM modes). Interestingly, when the reaction with PGA was conducted at a higher concentration (10 μM of probe **10** *vs.* 1 μM for fluorescence-based assays), we also observed the formation of a minor side-product (*ca.* 15%) identified as the pyronin **13** substituted at the *meso*-position (*i.e.*, C-9 position) by edaravone (t_R = 4.0 min, MS(ESI+): m/z = 439.3 $[M + H]^+$, calcd for $C_{27}H_{27}N_4O_2^+$ 439.2 and UV-vis: λ_{max} = 538 nm). This unexpected result confirms both the moderate electrophilic reactivity of the C-9 position of pyronins and nucleophilicity of edaravone in its deprotonated form, under aqueous physiological conditions. To the best of our knowledge, **10** is the first example of the "covalent-assembly" type probe whose enzymatic activation leads to the simultaneous formation of a xanthene-based fluorophore and release of a bioactive substance. Indeed, the only two examples of such fluorogenic prodrugs are nitroreductase (NTR)-sensitive caged precursors namely **GMC-CA$_E$-NO$_2$** (Fig. 4A) and **FDU-DB-NO$_2$** (Fig. 4B) whose activation under hypoxic conditions (and subsequent UV-irradiation for **GMC-CA$_E$-NO$_2$**) produces a blue or green emitting 7-*N*,*N*-diethylaminocoumarin derivative and a cytotoxic cancer chemotherapy

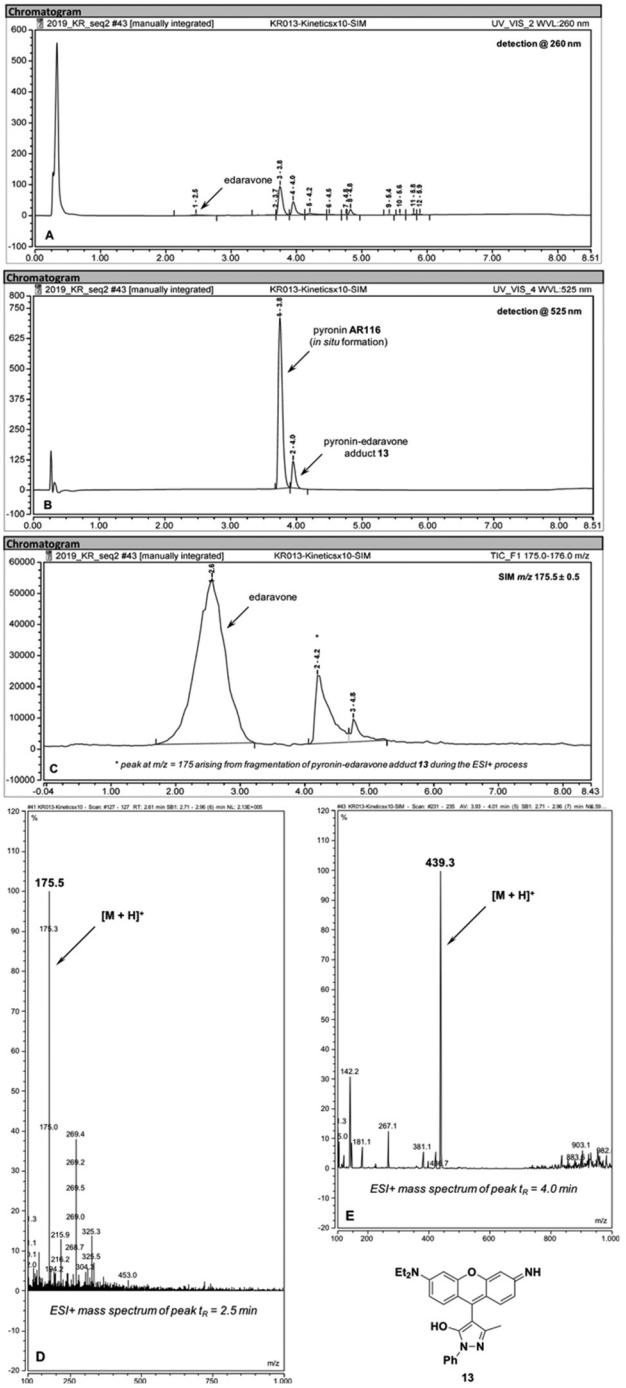

Fig. 3 RP-HPLC elution profiles (UV-vis and ESI+ mass detection, system B) of the enzymatic reaction mixture of probe **10** with PGA (20 h of incubation in PB at 37 °C). (A) UV detection at 260 nm, (B) visible detection at 525 nm, (C) ESI+ mass detection in the SIM mode, (D) ESI+ mass spectrum of the released edaravone and (E) ESI+ mass spectrum of pyronin–edaravone adduct **13**.

agent (gemcitabine and floxuridine respectively) for bioimaging, tracking drug release and anticancer application.[24] In this context, a slow liberation of drug molecules may be advantageous to reduce the "burst effect" which is the primary source of severe side-effects associated with such therapeutic treatments.[25]

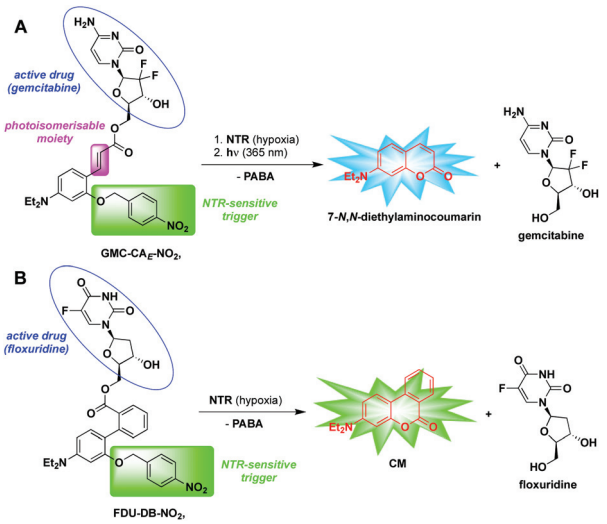

Fig. 4 Hypoxia-activated anticancer theranostic prodrugs based on the "covalent-assembly" strategy and already reported in the literature.[24]

The assumed PGA sensing mechanism for rosamine-based pro-fluorophore **7** is dramatically different and based on the more conventional enzyme-mediated aniline deprotection process.[1a,26] Since the released pyronin–coumarin hybrid dye has never been reported in the literature, its photophysical properties and ability to display an internal energy transfer process[27] or PeT quenching[28] are not known. Therefore, the kinetic fluorescence measurements of PGA activation at Ex./Em. 525/545 nm did not show a detectable "turn-on" response (Fig. 1). In order to identify the primary factor behind this negative outcome (*i.e.*, wrong detection parameters or poor substrate of PGA), fluorescence emission and excitation spectra in the wavelength ranges anticipated for these coumarin and pyronin chromophores have been recorded after 30 min incubation of probe **7** with PGA (see Fig. S13‡). The shape and position of the emission band (centered at 560 nm) are consistent with a xanthene dye. The excitation spectrum of the emissive species causing this yellow fluorescence displays a single band centered at 535 nm. This indicates no direct π-conjugation in the ground state between these two chromophores that take up a perpendicular geometry to each other, and no energy transfer between them. We have therefore performed a second kinetic experiment with the optimized set of Ex./Em. 535/560 nm parameters and the expected fluorogenic "turn-on" response was observed (190 AFU within 30 min, Fig. 5). However, the low level of fluorescence reached suggests a poor quantum yield for the released rosamine **14** that can be explained in part by a tautomeric equilibrium with a weakly (or non-) fluorescent species (Fig. 5).[29]

This comparative study concludes with reactions between the PGA enzyme and hemicyanine-like derivatives **8** and **9** and for which no significant increase in pyronin fluorescence within the time range of 30 min was observed. Theoretically, two possible interpretations can be put forth

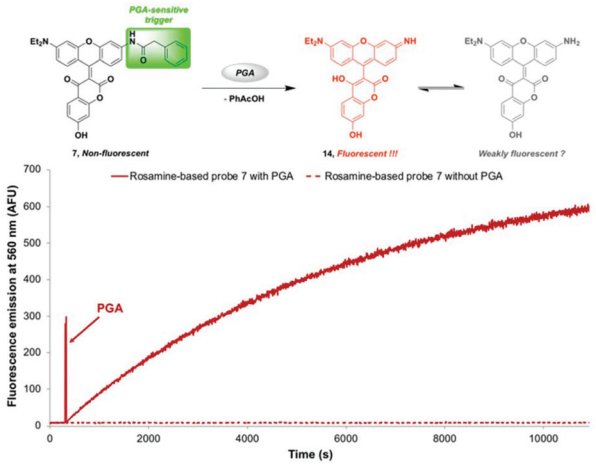

Fig. 5 Fluorescence-based PGA assay with pyronin–coumarin hybrid pro-fluorophore **7**. (Top) Activation mechanism based on the deprotection of fluorogenic primary aniline and possible tautomeric equilibrium, (bottom) time-dependent changes in the yellow fluorescence intensity (Ex./Em. 535/560 nm, slit 5 nm) of fluorogenic probe **7** (concentration: 1.0 μM) in the presence of PGA (1 U) in PB (100 mM, pH 7.6) at 37 °C. Please note: PGA was added after 5 min of incubation of probe in PB alone.

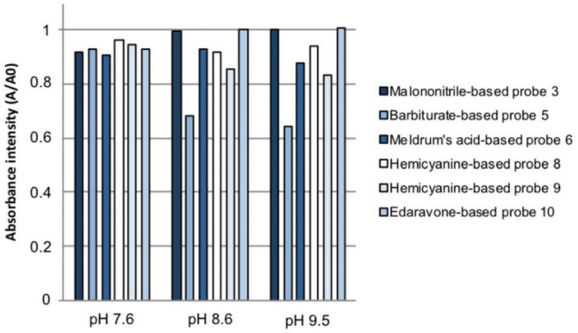

Fig. 6 UV-vis absorbance changes (at λ_{max}) of fluorogenic probes **3**, **5**, **6**, **8**, **9** and **10** after 30 min incubation in three distinct aqueous buffers (PB, 100 mM, pH 7.6 and borate buffer, 100 mM, pH 8.6 and 9.5) at 25 °C (concentration: 2.0 μM).

to explain these results: (1) undesired conversion of the hemicyanine-based Michael acceptor moiety into a less reactive aldehyde functionality through the retro-Knoevenagel reaction, known to be favoured in basic aqueous media and already reported for some cyanine dyes[30] and/or the (2) poor leaving group ability of the *N*-quaternised aza-heterocycle bearing an activated methyl group that directly affects the rate of the 1,6-elimination process. Since, we did not observe any change (*i.e.*, blue-shift of the absorption maximum and the hypochromic effect in line with the loss of an extended π system) in the UV-vis absorption spectra of **8** and **9** during their incubation in phosphate buffer (see bar charts shown in Fig. 6), the second hypothesis is preferred. Unfortunately, the pK_a values of active methyl compounds 1,4-dimethylpyridinium and 1-ethyl-2,3,3-trimethylindolenium (iodide salts) are not available to further support our hypothesis. All the same, we may conclude that *N*-quaternised aza-heterocycles bearing an activated methyl group are not suitable candidates to promote the activation kinetics of pyronin caged precursors.

The *in situ* formation of pyronin **AR116** in samples from enzymatic fluorescence assays was further confirmed by RP-HPLC (coupled with fluorescence detection) analyses, including the comparison of the observed retention time (t_R = 3.8 min) with that of an authentic sample of synthetic pyronin **AR116** used as a reference (see Fig. S21–S37‡ for the RP-HPLC elution profiles). By analogy with our previous observations made during fluorescent enzyme assays with aldehyde-based "covalent-assembly" probe **2**, a second fluorescent species identified as mono-dealkylated pyronin was observed but only on the RP-HPLC-fluorescence elution profile (t_R = 3.5 min) of the crude enzymatic reaction of hemicyanine-like derivative **9**. Since this probe exhibits the highest ability to absorb visible light (*vide supra*), we assume that the photooxidative *N*-dealkylation process leading to photobluing of fluorescent organic dyes bearing (di)alkylamino auxochromic groups,[31] such as pyronin **AR116**, occurs upon prolonged illumination at 525 nm implemented during the fluorescence-based *in vitro* assays.

Aqueous stability and thiol-reactivity of Michael acceptor-based caged precursors

Since the undesired reaction of Michael acceptor-based caged precursors with hydroxide ions, water or biological nucleophiles would lead either to adducts not prone to cyclisation–elimination to yield the pyronin or to the premature release of the second molecule of interest (*e.g.*, drugs such as barbiturates or edaravone) through the retro-Knoevenagel reaction, it was essential to conduct further studies to assess the pH-dependent stability of these probes and their possible reaction with biothiols. On the basis of the findings of *in vitro* enzymatic assays, the most promising probes **3**, **5**, **6** and **10** have been selected and subjected to incubation in three different aqueous buffers (*i.e.*, phosphate pH 7.6, borate pH 8.5 and 9.5). Monitoring of absorbance at their maximum wavelength (in the range of 445–490 nm) over time, which is assumed to be lost upon the nucleophilic addition of a water molecule or hydroxide ion and possibly retro-Knoevenagel reaction leading to conversion to the corresponding aldehyde (bathochromic shift), is a simple way to rapidly check the overall stability of these Michael acceptor-based caged precursors. It could be seen that there were negligible absorbance changes for probes **3**, **6** and **10** at all pH values (see bar charts shown in Fig. 6), indicating their good aqueous stability. Conversely, a significant decrease in absorbance at 490 nm was observed for the probe bearing a methylidene 1,3-dimethylbarbituric acid portion, upon an increase of pH from 7.6 to 9.5. For practically equivalent performance in fluorogenic "turn-on" response, it would then be preferable to use a dicyanomethylidenyl or methylidene Meldrum's acid moiety rather than the more reac-

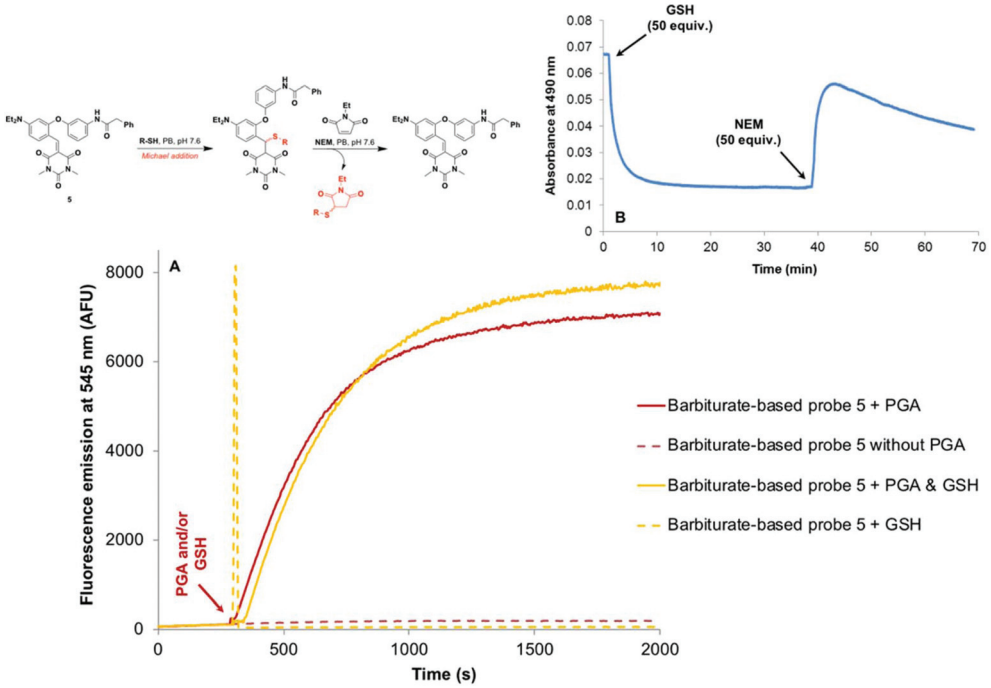

Fig. 7 Thiol reactivity of barbiturate-based probe **5** in PB (100 mM, pH 7.6). (A) Time-dependent changes in the green-yellow fluorescence intensity (Ex./Em. 525/545 nm, slit 5 nm) of **5** (concentration: 1.0 μM) in the presence of PGA (1 U) with or without glutathione (GSH = R-SH, 50 equiv.) at 37 °C. Please note: PGA was added after 5 min of incubation of probe in PB alone. (B) Time-dependent changes in absorbance (490 nm) of **5** (concentration: 2.0 μM) after sequential addition of GSH (50 equiv.) and NEM (50 equiv.) at 25 °C. (GSH = glutathione, NEM = *N*-ethylmaleimide).

tive Michael acceptor namely methylidene 1,3-dimethylbarbituric acid.

The other important feature for considering the use of such probes in complex biological media is their chemical inertness toward biothiols such as glutathione (GSH) whose concentration could reach high values, especially in tumor cells (0.5–10 mM).[32] In this context, further fluorescence PGA assays and absorbance measurements were performed in phosphate buffer (pH 7.6) and in the presence of 50 equiv. of GSH. Gratifyingly, no deleterious effect of GSH on the fluorogenic "turn-on" response and hence on the *in situ* pyronin formation process was observed (see Fig. 7A and Fig. S17–S19‡). Perhaps more surprising are the results obtained with barbiturate-based probe **5**. Indeed, a rapid and dramatic decrease of its absorption at 490 nm was observed, confirming that the thiol-Michael addition reaction occurred (see Fig. 7B and bar charts shown in Fig. S20‡). However, the apparent disappearance of the Michael acceptor moiety is not likely to negatively impact the tandem cyclisation–aromatisation process yielding a pyronin structure, because the level of fluorescence achieved after 30 min incubation of probe **5** with PGA and GSH is higher than that obtained with the enzymatic reaction conducted without this thiol additive (Fig. 7A). This surprising result can be potentially explained by the reversibility of the GSH-probe adduct, demonstrated by a further experiment in which the probe **5** was sequentially incubated with GSH (50 equiv.) and *N*-ethylmaleimide (NEM, 50 equiv.).[33] Indeed, the addition of an equimolar amount of this thiol scavenger has led to the resurgence of the visible absorbance feature of **5** (Fig. 7B). We can conclude that thiols may be protective for Michael acceptor-based caged precursors by preventing their hydration and subsequent conversion to less reactive aldehyde derivative **2** through the retro-Knoevenagel reaction. This feature is particularly valuable for biomedical applications in living systems.

Conclusions

In summary, a significant advance has been made both to fine-tune the reactivity and optimise the properties of "covalent-assembly" type probes that utilise the targeted enzyme to build a detectable pyronin fluorophore under physiological conditions. Indeed, the change of the Michael acceptor moiety involved in the domino cyclisation–aromatisation reaction leading to a xanthene scaffold was identified as a subtle but effective structural modification to dramatically impact the kinetics of this unusual protease-triggered fluorogenic process. Indeed, in the context of our fluorescence-based bioassay format, Michael acceptor adducts derived from C-nucleophiles, namely 1,3-dimethylbarbituric acid, malononitrile and Meldrum's acid, are quantitatively converted into pyronin **AR116** within 30 min of incubation with PGA at physiological pH. The enhanced intensity and shortened time-scale of the resulting fluorogenic "turn-on" response are first steps toward the future implementation of such a "covalent-assembly" strat-

egy towards spatio-temporal profiling of disease-relevant enzymes in live cells and *in vivo*. We also demonstrated that the apparent discrepancy between the reactivity and aqueous stability of these probes related to the enhanced electrophilicity of their Michael acceptor moiety could be dismissed out of hand by the protective effect of biothiols demonstrated through *in vitro* assays conducted with GSH. This trick cannot, however, be used for the dimedone-based "covalent-assembly" type probe **4** because of its marked chemical instability. The high electrophilicity of the corresponding Michael acceptor and the good leaving group ability of dimedone are insurmountable obstacles to the further use of this moiety as an effective promoter of activation kinetics of this unusual class of enzyme-responsive fluorogenic probes. Interestingly, the *in situ* formation of fluorescent pyronin **AR116** at a slower rate was achieved with a pyrazolone-based Michael acceptor **10** (*i.e.*, edaravone as a C-nucleophile). In this latter case, pyronin formation is accompanied by the release of edaravone as demonstrated by HPLC-MS analyses. This strategy could provide a novel and promising platform for the facile construction of theranostic prodrugs activated by enzymes or reactive bioanalytes associated with a specific disease.[13] Indeed, the versatile synthetic route toward mixed bis-aryl ether derivatives devised by us could be used by changing only the analyte-sensitive trigger group and C-nucleophile. However, we are fully aware that the bioactive molecule chosen for the construction of such fluorogenic theranostic conjugates must bear an easily enolisable position or be functionalised with a C-nucleophile having low pK_a and that does not negatively affect its biological properties. Moreover, Knoevenagel condensation with fluorescent organic dyes bearing an enolisable carbon should enable the rapid development of two-channel fluorescent probes with a more sophisticated signaling mechanism,[34] especially for the simultaneous detection of two distinct (bio)analytes.[6a,35] For such a purpose, a possible and straightforward strategy would be to perform Knoevenagel condensation with a cyclic C-nucleophile that contains an additional group (*e.g.*, amino or azido group, carboxylic acid, terminal alkyne, *etc.*)[36] suitable for its covalent conjugation to a pro-fluorophore sensitive to the second targeted (bio)analyte (Fig. 8).

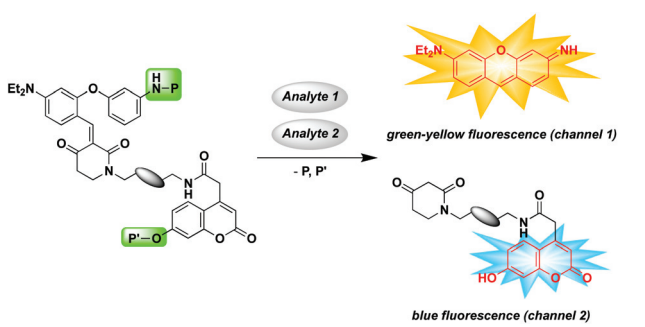

Fig. 8 A possible strategy toward double-emission fluorescent probe for discriminatory detection of two distinct analytes, based on the conjugation of a "covalent-assembly" type probe to a conventional phenol-based pro-fluorophore (*e.g.*, 7-hydroxycoumarin-4-acetic acid) through a functionalised cyclic C-nucleophile.

Experimental section

For all experimental details related to photophysical characterisation, fluorescence-based *in vitro* assays and HPLC-fluorescence/-MS analyses, see the ESI.‡

General

Unless otherwise noted, all commercially available reagents and solvents were used without further purification. TLC was carried out on Merck DC Kieselgel 60 F-254 aluminum sheets. The spots were directly visualised or through illumination with a UV lamp (λ = 254/365 nm) and/or staining with $KMnO_4$ solution. Purifications by flash column chromatography were performed on silica gel (40–63 μm) from VWR. Anhydrous DMSO was purchased from Carlo Erba, and stored over 3 Å molecular sieves. Absolute EtOH (+99.8%, Reag. Ph. Eur. for analyses) was purchased from VWR. Piperidine (peptide grade, SOL-010) and PGA (from *Escherichia coli*, EZ50150, 841 U mL^{-1}) were provided by Iris Biotech GmbH. Formic acid (FA, puriss p.a., ACS reagent, reag. Ph. Eur., ≥98%), 4,7-dihydroxycoumarin (97%) and DMSO (molecular biology grade) were provided by Sigma-Aldrich. Edaravone, *N*-ethylmaleimide (NEM) and glutathione (reduced form, GSH, 98%) were purchased from Rhone-Poulenc Rorer, Pierce and Acros respectively. The HPLC-gradient grade acetonitrile (MeCN) was obtained from Carlo Erba or VWR. All aqueous buffers used in this work and aqueous mobile-phases for HPLC were prepared using water purified with a PURELAB Ultra system from ELGA (purified to 18.2 MΩ cm). Aldehyde- and dicyanomethylidene-based PGA probes [2097130–07–7] **2** and [2305970–99–2] **3**, 1,4-dimethylpyridinium iodide [2301–80–6] and 1-ethyl-2,3,3-trimethylindolenium iodide [14134–81–7] were prepared according to the literature procedures.[8w,10,14,37]

Instruments and methods

Freeze-drying operation was performed with a Christ Alpha 2–4 LD plus. Centrifugation steps were performed with a Thermo Scientific Espresso Personal Microcentrifuge instrument. ^{1}H-, ^{13}C- and ^{19}F-NMR spectra were recorded either on a Bruker Avance III 500 MHz or on a Bruker Avance III HD 600 MHz spectrometer (equipped with double resonance broad band probes). Chemical shifts are expressed in parts per million (ppm) from the residual non-deuterated solvent signal.[38] *J* values are expressed in Hz. IR spectra were recorded with a Bruker Alpha FT-IR spectrometer equipped with a universal ATR sampling accessory. The bond vibration frequencies are expressed in reciprocal centimeters (cm^{-1}). HPLC-MS analyses were performed on a Thermo-Dionex Ultimate 3000 instrument (pump + autosampler at 20 °C + column oven at 25 °C) equipped with a diode array detector (Thermo-Dionex DAD 3000-RS) and an MSQ Plus single quadrupole mass spectrometer. HPLC-fluorescence analyses were performed with the same instrument coupled to a RS fluorescence detector (Thermo-Dionex, FLD 3400-RS). Purifications by semi-preparative HPLC were performed on a Thermo-Dionex Ultimate 3000 instrument (semi-preparative pump HPG-3200BX)

equipped with an RS Variable Detector (VWD-3400RS, four distinct wavelengths within the range 190–900 nm). Ion chromatography analyses (for TFA quantification) were performed using a Thermo Scientific Dionex ICS 5000 ion chromatograph equipped with a conductivity detector CD (Thermo Scientific Dionex) and a conductivity suppressor ASRS-ultra II 4 mm (Thermo Scientific Dionex). Low-resolution mass spectra (LRMS) were recorded on a Thermo Scientific MSQ Plus single quadrupole equipped with an electrospray (ESI) source (direct introduction or LC-MS coupling). High-resolution mass spectra (HRMS) were recorded on a Thermo LTQ Orbitrap XL apparatus equipped with an ESI source.

High-performance liquid chromatography separations

Several chromatographic systems were used for the analytical experiments (HPLC-MS or HPLC-fluorescence) and the purification steps: *System A*: RP-HPLC-MS (Phenomenex Kinetex C_{18} column, 2.6 μm, 2.1 × 50 mm) with MeCN (+0.1% FA) and 0.1% aqueous formic acid (aqueous FA, pH 2.7) as eluents [5% MeCN (0.1 min) followed by linear gradient from 5% to 100% (5 min) of MeCN] at a flow rate of 0.5 mL min^{-1}. UV-visible detection was achieved at 220, 260, 450 and 500 nm (+diode array detection in the range of 220–700 nm). Low resolution ESI-MS detection in the positive/negative mode (full scan, 100–1000 a.m.u., data type: centroid, needle voltage: 3.0 kV, probe temperature: 350 °C, cone voltage: 75 V and scan time: 1 s). *System B*: system A with UV-visible detection at 220, 260, 470 and 525 nm (+diode array detection in the range of 220–800 nm). Low resolution ESI-MS detection in the positive/negative mode (full scan, 100–1000 a.m.u. and SIM mode with the following mass range (m/z 175.5 ± 0.5)). *System C*: system A with ultrapure H_2O and MeCN (without FA additive) as eluents. *System D*: semi-preparative RP-HPLC (SiliCycle SiliaChrom C_{18} column, 10 μm, 20 × 250 mm) with MeCN and ultrapure H_2O as eluents [25% MeCN (5 min), followed by a gradient of 25% to 55% MeCN (10 min), then 55% to 100% MeCN (45 min)] at a flow rate of 20.0 mL min^{-1}. Quadruple UV-vis detection was achieved at 220, 260, 460 and 550 nm. *System E*: system D with UV-visible detection at 220, 260, 470 and 530 nm. *System F*: system D with UV-visible detection at 220, 260, 280 and 475 nm. *System G*: system D with the following gradient [30% MeCN (5 min), followed by a gradient of 30% to 60% MeCN (10 min), then 60% to 100% MeCN (40 min)] at a flow rate of 20.0 mL min^{-1}. Quadruple UV-vis detection was achieved at 220, 260, 350 and 470 nm. *System H*: semi-preparative RP-HPLC (SiliCycle SiliaChrom C_{18} column, 10 μm, 20 × 250 mm) with MeCN and aqueous 0.1% TFA (pH 2.0) as eluents [10% MeCN (5 min), followed by a gradient of 10% to 30% MeCN (10 min), then 30% to 100% MeCN (95 min)] at a flow rate of 20.0 mL min^{-1}. Quadruple UV-vis detection was achieved at 220, 260, 500 and 550 nm. *System I*: system H with the following gradient [25% MeCN (5 min), followed by a gradient of 25% to 45% MeCN (10 min), then 45% to 100% MeCN (75 min)] at a flow rate of 20.0 mL min^{-1}. Quadruple UV-vis detection was achieved at 220, 260, 350 and 550 nm. *System J*: RP-HPLC-fluorescence (Phenomenex Kinetex C_{18} column, 2.6 μm, 2.1 × 50 mm) with the same eluents and gradient as system A. Fluorescence detection was achieved at 45 °C at the following Ex./Em. channels: 525/545 nm, 510/530 nm and 440/600 nm (sensitivity: 1, PMT 1, filter wheel: auto).

General procedure for the synthesis of Michael acceptor-based caged precursors. To a stirred solution of aldehyde **2** (40 mg, 0.1 mmol, 1 equiv.) in absolute EtOH (5 mL), C-nucleophile (0.105 mmol, 1.05 equiv.), anhydrous Na_2SO_4 (10 mg) and piperidine (1 drop) were successively added. The resulting reaction mixture was stirred for a defined duration and temperature depending on the C-nucleophile used. After completion of the reaction, the mixture was evaporated under reduced pressure and the resulting residue was directly purified by flash-column chromatography over silica gel (*ca.* 12 g). Further purification by semi-preparative RP-HPLC was achieved to obtain the desired PGA-sensitive probe with a purity >95% required for fluorescence measurements and enzymatic assays.

Dimedone-based PGA-sensitive probe (4). Dimedone was used as a C-nucleophile (14.7 mg, 0.105 mmol, 1.05 equiv.). The reaction mixture was stirred at RT overnight and under reflux for 1 h. The crude product was purified by flash-column chromatography (step gradient of EtOAc in heptane from 40% to 100%) and semi-preparative RP-HPLC (system F, t_R = 37.5–39.5 min). The desired PGA-sensitive probe **4** was recovered (after freeze-drying) as a red amorphous powder (*ca.* 0.1 mg, <1 μmol, yield <1%). *Please note: This compound was found to be too unstable to be isolated in significant amounts required for ^1H and ^{13}C NMR analyses*. IR (ATR): ν = 2923, 2853, 2319, 2221, 2197, 2176, 2161, 2073, 2049, 2038, 2003, 1991, 1974, 1736, 1707, 1611, 1508, 1458, 1377, 1350, 1260, 1111, 1027, 796, 669 cm^{-1}; *please note: partial degradation of the product was noted during the RP-HPLC analysis conducted with or without the FA additive.* HPLC (system C): t_R = 5.6 min; LRMS (ESI+, recorded during RP-HPLC analysis): m/z 525.4 $[M + H]^+$ (100), calcd for $C_{33}H_{37}N_2O_4^+$ 525.3; LRMS (ESI−, recorded during RP-HPLC analysis): m/z 523.2 $[M - H]^-$ (100), calcd for $C_{33}H_{35}N_2O_4^-$ 523.3; HRMS (ESI+): m/z 525.27370 $[M + H]^+$, calcd for $C_{33}H_{37}N_2O_4^+$ 525.27478, and 547.25662 $[M + Na]^+$, calcd for $C_{33}H_{36}N_2O_4Na^+$ 547.25673; UV-vis: λ_{max} (PB)/nm 281 and 495 (ε/dm^3 mol^{-1} cm^{-1} 20 700 and 11 900).

Barbiturate-based PGA-sensitive probe (5). 1,3-Dimethylbarbituric acid was used as a C-nucleophile (16.4 mg, 0.105 mmol, 1.05 equiv.). The reaction mixture was stirred at RT overnight. The crude product was purified by flash-column chromatography (step gradient of MeOH in DCM from 0% to 20%) and semi-preparative RP-HPLC (system E, t_R = 32.0–35.0 min). The desired PGA-sensitive probe **5** was recovered (after freeze-drying) as an orange amorphous powder (30.9 mg, 57 μmol, yield 57%). IR (ATR): ν = 3253, 2971, 2066, 1710, 1650, 1609, 1527, 1501, 1419, 1387, 1371, 1342, 1306, 1266, 1196, 1169, 1072, 968, 872, 824, 786, 756, 708, 679, 653 cm^{-1}; ^1H NMR (500 MHz, $CDCl_3$): δ = 9.09–8.83 (m, 2 H), 7.42–7.35 (m, 3 H), 7.34–7.29 (m, 3 H), 7.26–7.18 (m, 2 H), 7.12 (d, J = 2.2 Hz, 1 H), 6.75–6.67 (m, 1 H), 6.45 (dd, J = 9.6, J = 2.7 Hz, 1 H), 5.97 (d, J = 2.7 Hz, 1 H), 3.70 (s, 2 H), 3.39

(s, 3 H), 3.37–3.30 (m, 7 H), 1.12 (t, J = 7.1 Hz, 6 H) ppm; ^{13}C NMR (126 MHz, $CDCl_3$): δ = 169.2, 164.3, 162.9, 161.9, 156.7, 154.7, 152.1, 151.8, 139.4, 137.3, 134.5, 130.2, 129.6, 129.4, 127.8, 115.6, 115.3, 112.7, 111.3, 109.3, 106.8, 99.4, 45.2, 45.0, 28.9, 28.37, 12.8 ppm; *please note: partial degradation of the product was noted during the RP-HPLC analysis conducted with or without the FA additive.* HPLC (system C): t_R = 5.4 min (purity 74% at 260 nm, 90% at 450 nm and 76% at 500 nm); LRMS (ESI+, recorded during RP-HPLC analysis): m/z 541.3 $[M + H]^+$ (100), calcd for $C_{31}H_{33}N_4O_5^+$ 541.2; LRMS (ESI−, recorded during RP-HPLC analysis): m/z 539.0 $[M - H]^-$ (100), calcd for $C_{31}H_{31}N_4O_5^-$ 539.2; HRMS (ESI+) m/z 541.24545 $[M + H]^+$, calcd for $C_{31}H_{33}N_4O_5^+$ 541.24455, and 563.22691 $[M + Na]^+$, calcd for $C_{31}H_{32}N_2O_6Na^+$ 563.22649; UV-vis: λ_{max} (PB)/nm 251 and 493 (ε/dm^3 mol^{-1} cm^{-1} 29 800 and 31 600).

Meldrum's acid-based PGA-sensitive probe (6). Meldrum's acid was used as a C-nucleophile (15.1 mg, 0.105 mmol, 1.05 equiv.). The reaction mixture was stirred at RT for 5 h. The crude product was purified by flash-column chromatography (step gradient of MeOH in DCM from 0% to 10%) and semi-preparative RP-HPLC (system D, t_R = 32.0–33.5 min). The desired PGA-sensitive probe **6** was recovered as a red amorphous powder (25.2 mg, 47 μmol, yield 47%). IR (ATR): ν = 3315, 3087, 2976, 2933, 1685, 1602, 1542, 1499, 1436, 1376, 1346, 1297, 1256, 1177, 1121, 1095, 1075, 1003, 958, 932, 892, 826, 789, 757, 722, 695, 684, 645 cm^{-1}; ^{1}H NMR (500 MHz, $CDCl_3$): δ = 9.26 (d, J = 1.9 Hz, 1 H), 9.11 (dd, J = 9.5 Hz, J = 1.9 Hz, 1 H), 7.99 (s, 1 H), 7.77–7.65 (m, 5 H), 7.65–7.56 (m, 3 H), 7.06 (d, J = 7.5 Hz, 1 H), 6.90–6.65 (m, 1 H), 6.26 (t, J = 2.2 Hz, 1 H), 4.06 (d, J = 2.5 Hz, 2 H), 3.67 (q, J = 7.3 Hz, 4 H), 2.12 (t, J = 1.5 Hz, 6 H), 1.46 (td, J = 7.3 Hz, J = 4.0 Hz, 6H) ppm; ^{13}C NMR (126 MHz, $CDCl_3$): δ = 169.4, 165.6, 165.6, 163.0, 156.1, 156.0, 154.8, 150.9, 139.6, 136.6, 134.6, 130.1, 129.6, 129.2, 127.7, 115.8, 115.6, 111.7, 111.6, 107.2, 103.5, 98.7, 98.6, 45.2, 44.8, 27.4, 12.7 ppm; HPLC (system A): t_R = 5.4 min (purity 95% at 260 nm, 99% at 450 nm and 85% at 500 nm); LRMS (ESI+, recorded during RP-HPLC analysis): m/z 529.2 $[M + H]^+$ (100), calcd for $C_{31}H_{33}N_2O_6^+$ 559.2; LRMS (ESI−, recorded during RP-HPLC analysis) m/z 527.3 $[M - H]^-$ (100), calcd for $C_{31}H_{31}N_2O_6^-$ 557.2; HRMS (ESI+) m/z 529.23410 $[M + H]^+$, calcd for $C_{31}H_{33}N_2O_6^+$ 559.23331, and 551.21596 $[M + Na]^+$, calcd for $C_{31}H_{33}N_2O_6Na^+$ 551.21526; UV-vis: λ_{max} (PB)/nm 254, 286, 487 (ε/dm^3 mol^{-1} cm^{-1} 23 000, 15 100 and 29 500); fluorescence λ_{max} (PB)/nm 612 (Φ_F 1%).

Rosamine-based PGA-sensitive probe (7). 4,7-Dihydroxycoumarin was used as a C-nucleophile (18.7 mg, 0.105 mmol, 1.05 equiv.). The reaction mixture was stirred under reflux for 3 h. The crude product was purified by flash-column chromatography (step gradient of MeOH in DCM from 0% to 10%) and semi-preparative RP-HPLC (system H, t_R = 38.0–40.0 min). TFA salt of the desired PGA-sensitive probe **7** was recovered (after freeze-drying) as a dark purple amorphous powder (7.0 mg, 10 μmol, yield 10%). IR (ATR): ν = 2981, 1673, 1641, 1589, 1506, 1451, 1346, 1308, 1264, 1235, 1195, 1159, 1128, 1073, 1007, 989, 948, 824, 798, 772, 749, 704, 652 cm^{-1}; ^{1}H NMR (600 MHz, DMSO-d_6): δ = 11.02 (s, 1 H), 10.14 (s, 1 H), 8.32 (d, J = 2.0 Hz, 1 H), 7.93 (d, J = 9.1 Hz, 1 H), 7.81 (d, J = 9.7 Hz, 1 H), 7.70 (d, J = 8.5 Hz, 1 H), 7.43 (dd, J = 9.1 Hz, J = 2.0 Hz, 1 H), 7.40–7.31 (m, 3 H), 7.31–7.21 (m, 2 H), 7.05 (d, J = 2.4 Hz, 1 H), 6.66 (dd, J = 8.4 Hz, J = 2.4 Hz, 1 H), 6.58 (t, J = 2.9 Hz, 1 H), 3.78 (s, 2 H), 3.72 (q, J = 7.1 Hz, 4 H), 1.54–0.96 (m, 6 H) ppm; ^{13}C NMR (151 MHz, DMSO-d_6): δ = 171.1, 171.0, 162.4, 161.4, 158.9, 157.2, 156.1, 155.3, 146.6, 135.6, 135.3, 132.7, 129.8, 128.9, 127.2, 118.1, 117.7, 117.3, 115.9, 111.7, 104.8, 102.0, 101.9, 95.7, 92.2, 46.1, 43.9, 43.8 ppm; ^{19}F NMR (565 MHz, DMSO-d_6): δ = −73.5 (s, 3 F, CF_3-TFA) ppm; HPLC (system A): t_R = 4.2 min (purity >99% at 260 nm, >99% at 450 nm and >99% at 500 nm); LRMS (ESI+, recorded during RP-HPLC analysis): m/z 561.3 $[M + H]^+$ (100), calcd for $C_{34}H_{29}N_2O_6^+$ 561.2; LRMS (ESI−, recorded during RP-HPLC analysis): m/z 559.1 $[M - H]^-$ (100), calcd for $C_{34}H_{27}N_2O_6^-$ 559.2; HRMS (ESI+): m/z 561.20278 $[M + H]^+$, calcd for $C_{34}H_{29}N_3O_6^+$ 561.20201, and 583.18333 $[M + Na]^+$, calcd for $C_{34}H_{28}N_3O_6Na^+$ 583.18396; UV-vis: λ_{max} (PB)/nm 303, 507 and 552 (ε/dm^3 mol^{-1} cm^{-1} 39 000, 36 900 and 34 800).

Hemicyanine-based PGA-sensitive probe (8). 1,4-Dimethylpyridinium iodide was used as a C-nucleophile (24.7 mg, 0.105 mmol, 1.05 equiv.). The reaction mixture was stirred under reflux for 6 h. The crude product was purified by flash-column chromatography (eluent: DCM–EtOAc, 8 : 2 (v/v) then DCM–MeOH, 95 : 5, v/v) and semi-preparative RP-HPLC (system H, t_R = 36.0–43.0 min). TFA salt of the desired PGA-sensitive probe **8** was recovered (after freeze-drying) as a red amorphous powder (22.5 mg, 37 μmol, yield 37%). IR (ATR): ν = 3259, 3061, 2973, 2931, 2630, 2067, 1670, 1645, 1573, 1518, 1418, 1481, 1454, 1436, 1404, 1378, 1353, 1340, 1305, 1272, 1238, 1226, 1177, 1124, 1093, 1075, 1043, 961, 871, 821, 796, 717, 695, 685 cm^{-1}; ^{1}H NMR (500 MHz, $CDCl_3$): δ = 9.46 (s, 1 H), 8.26–7.96 (m, 2 H), 7.61 (d, J = 15.9 Hz, 1 H), 7.46 (s, 1 H), 7.40 (d, J = 8.9 Hz, 1 H), 7.34 (s, 2 H), 7.23 (d, J = 6.9 Hz, 3 H), 7.15 (t, J = 7.4 Hz, 2 H), 7.08 (q, J = 8.6 Hz, J = 8.1 Hz, 2H), 6.65 (d, J = 15.9 Hz, 1 H), 6.53 (d, J = 8.1 Hz, 1 H), 6.35 (d, J = 8.8 Hz, 1 H), 6.00 (s, 1 H), 3.88 (s, 3 H), 3.63 (s, 2 H), 3.20 (q, J = 7.1 Hz, 4 H), 1.01 (t, J = 7.1 Hz, 6 H) ppm; ^{13}C NMR (126 MHz, $CDCl_3$): δ = 170.5, 158.4, 157.2, 154.6, 151.7, 143.4, 140.6, 137.4, 135.6, 130.4, 130.0, 129.6, 128.7, 127.1, 122.3, 116.5, 115.5, 113.5, 113.4, 110.8, 108.3, 101.7, 46.6, 44.9, 44.2, 12.7, 1.2 ppm; ^{19}F NMR (470 MHz, $CDCl_3$): δ = −75.3 (s, 3 F, CF_3–TFA) ppm; HPLC (system A): t_R = 4.5 min (purity >99% at 260 nm, >99% at 450 nm and 100% at 500 nm); LRMS (ESI+, recorded during RP-HPLC analysis): m/z 492.3 $[M]^{+\circ}$ (100), calcd for $C_{32}H_{33}N_3O_2^+$ 492.3; LRMS (ESI−, recorded during RP-HPLC analysis): m/z 536.0 $[M + FA - 2H]^-$ (40), calcd for $C_{33}H_{34}N_3O_4^-$ 536.3, and 582.2 $[M + 2FA - 2H]^-$ (100), calcd for $C_{34}H_{36}N_3O_6^-$ 582.3; HRMS (ESI+): m/z 492.26337 $[M]^{+\circ}$, calcd for $C_{32}H_{34}N_3O_2^+$ 492.26455; UV-vis: λ_{max} (PB)/nm 469 (ε/dm^3 mol^{-1} cm^{-1} 32 300).

Hemicyanine-based PGA-sensitive probe (9). 1-Ethyl-2,3,3-trimethylindolenium iodide was used as a C-nucleophile (33 mg, 0.105 mmol, 1.05 equiv.). The reaction mixture was stirred under reflux for 3 h. The crude product was purified by flash-column chromatography (step gradient of MeOH in DCM from

0% to 10%) and semi-preparative RP-HPLC (system I, t_R = 29.0–38.0 min). TFA salt of the desired PGA-sensitive probe **9** was recovered (after freeze-drying) as a purple amorphous powder (39.6 mg, 58 μmol, yield 58%). IR (ATR): ν = 3249, 3193, 3059, 3026, 2972, 2926, 2872, 2363, 2163, 2147, 2114, 2036, 1991, 1792, 1683, 1601, 1567, 1517, 1466, 1410, 1399, 1373, 1352, 1320, 1300, 1256, 1215, 1192, 1170, 1157, 1115, 1071, 1044, 1016, 981, 947, 926, 874, 821, 796, 757, 708, 694, 681 cm^{-1}; ^1H NMR (500 MHz, $CDCl_3$): δ = 10.84 (d, J = 5.8 Hz, 1 H), 8.34 (d, J = 15.2 Hz, 1 H), 7.90–7.73 (m, 2 H), 7.62 (dd, J = 8.1 Hz, J = 1.9 Hz, 1 H), 7.52–7.32 (m, 5 H), 7.31–7.18 (m, 4 H), 7.14 (dd, J = 8.4 Hz, J = 6.3 Hz, 1 H), 7.05 (d, J = 15.2 Hz, 1 H), 6.65 (dd, J = 8.1 Hz, J = 2.4 Hz, 1 H), 6.53 (dd, J = 9.3 Hz, J = 2.5 Hz, 1 H), 6.05 (d, J = 2.5 Hz, 1 H), 4.25 (q, J = 7.3 Hz, 2 H), 3.81 (s, 2 H), 3.34 (q, J = 7.2 Hz, 4 H), 1.59 (s, 6 H), 1.41 (t, J = 7.2 Hz, 3 H), 1.12 (t, J = 7.1 Hz, 6 H) ppm; ^{13}C NMR (126 MHz, $CDCl_3$): δ = 178.3, 171.1, 162.1, 161.2, 161.0, 155.6, 155.4, 149.4, 142.1, 142.0, 140.7, 136.2, 129.9, 129.7, 129.2, 128.3, 127.5, 126.5, 122.6, 118.8, 116.7, 116.4, 114.1, 113.2, 112.2, 111.2, 109.3, 103.1, 100.4, 50.8, 45.6, 44.0, 40.8, 27.8, 12.8, 12.7 ppm; ^{19}F NMR (470 MHz, $CDCl_3$): δ = −74.7 (s, 3 F, CF_3–TFA) ppm; HPLC (system A): t_R = 5.1 min (purity 97% at 260 nm, 96% at 450 nm and 98% at 500 nm); LRMS (ESI+, recorded during RP-HPLC analysis): m/z 572.5 $[M]^{+\circ}$ (100), calcd for $C_{38}H_{42}N_3O_2^+$ 572.3; LRMS (ESI−, recorded during RP-HPLC analysis): m/z 616.3 $[M + FA - 2H]^-$ (100), calcd for $C_{39}H_{42}N_3O_4^-$ 616.3, and 662.4 $[M + 2FA - 2H]^-$ (40), calcd for $C_{40}H_{44}N_3O_6^-$ 662.3; HRMS (ESI+): m/z 572.32597 $[M]^{+\circ}$, calcd for $C_{38}H_{42}N_3O_2^+$ 572.32715; UV-vis: λ_{max} (PB)/nm 548 (ε/dm^3 mol^{-1} cm^{-1} 67 900); fluorescence λ_{max} (PB)/nm 593 ($\Phi_F \ll 1\%$).

Edaravone-based PGA-sensitive probe (10). Edaravone was used as a C-nucleophile (18.3 mg, 0.105 mmol, 1.05 equiv.). The reaction mixture was stirred at RT for 90 min, and then under reflux for 2 h 30 min. The crude product was purified by flash-column chromatography (step gradient of EtOAc in DCM from 0% to 10%) and semi-preparative RP-HPLC (system G, t_R = 41.0–43.0 min). The desired PGA-sensitive probe **10** was recovered (after freeze-drying) as a red amorphous powder (10.3 mg, 18 μmol, yield 18%). IR (ATR): ν = 3298, 3064, 2974, 2042, 2003, 1667, 1599, 1573, 1544, 1515, 1497, 1455, 1436, 1413, 1375, 1352, 1333, 1307, 1270, 1202, 1148, 1099, 1077, 1024, 996, 963, 932, 863, 835, 766, 753, 721, 692, 670, 614 cm^{-1}; ^1H NMR (500 MHz, $CDCl_3$): δ = 9.58 (d, J = 9.3 Hz, 1 H), 7.94 (d, J = 8.0 Hz, 2 H), 7.73 (s, 1 H), 7.39 (d, J = 5.0 Hz, 1 H), 7.37–7.30 (m, 4 H), 7.26 (t, J = 6.5 Hz, 3 H), 7.24–7.21 (m, 2 H), 7.20 (d, J = 1.3 Hz, 1 H), 7.09 (t, J = 7.6 Hz, 1 H), 6.72 (dt, J = 7.3 Hz, J = 2.0 Hz, 1 H), 6.43 (dd, J = 9.4 Hz, J = 2.4 Hz, 1 H), 6.01 (d, J = 2.4 Hz, 1 H), 3.65 (s, 2 H), 3.27 (q, J = 7.2 Hz, 4 H), 2.15 (s, 3 H), 1.07 (t, J = 7.1 Hz, 6 H) ppm; ^{13}C NMR (126 MHz, $CDCl_3$): δ = 169.3, 163.1, 160.6, 157.7, 153.9, 151.8, 151.9, 140.2, 140.1, 139.5, 139.2, 136.8, 134.4, 130.2, 129.6, 129.3, 128.7, 127.8, 124.4, 120.3, 119.4, 115.1, 114.5, 113.31, 110.6, 107.6, 100.5, 45.1, 44.9, 13.5, 12.8 ppm; HPLC (system A): t_R = 6.1 min (purity 100% at 260 nm, 100% at 450 nm and 100% at 500 nm); LRMS (ESI+, recorded during RP-HPLC analysis): m/z 559.3 $[M + H]^+$ (100), calcd for $C_{35}H_{35}N_4O_3^+$ 559.3; HRMS (ESI+) m/z 559.27091 $[M + H]^+$, calcd for $C_{35}H_{35}N_4O_3^+$ 559.27037, 581.25261 $[M + Na]^+$, calcd for $C_{35}H_{34}N_4O_3Na^+$ 581.25231; UV-vis: λ_{max} (PB)/nm 257 and 486 (ε/dm^3 mol^{-1} cm^{-1} 29 500 and 29 700).

***N*-Boc-3-iodoaniline [143390–49–2] (11).** 3-Iodoaniline (2 g, 9.13 mmol, 1 equiv.) was dissolved in absolute EtOH (44 mL) and kept under an argon atmosphere. Boc_2O (2 g, 9.13 mmol, 1 equiv.) and TEA (2.54 mL, 18.26 mmol, 2 equiv.) were successively added and the resulting reaction mixture was stirred at RT overnight. The reaction was checked for completion by TLC (eluent: DCM 100%) and the mixture was then concentrated under reduced pressure. The resulting residue was dissolved in DCM (40 mL) and washed with aqueous 1.0 M HCl thrice. The organic layer was dried over anhydrous $MgSO_4$ and concentrated over reduced pressure to give *N*-Boc-3-iodoaniline **11** as a brown oily solid (2.26 g, 7.12 mmol, yield 78%). This product was directly used in the next step without further purification. R_f (DCM): 0.80; ^1H NMR (500 MHz, $CDCl_3$): δ = 7.83 (t, J = 1.8 Hz, 1 H), 7.35 (ddd, J = 7.9 Hz, J = 1.8 Hz, J = 1.0 Hz, 1 H), 7.33–7.22 (m, 1 H), 6.98 (t, J = 7.9 Hz, 1 H), 6.50 (s, 1 H), 1.51 (s, 9 H); ^{13}C NMR (126 MHz, $CDCl_3$): δ = 152.5, 139.7, 132.1, 130.5, 127.3, 117.7, 94.4, 28.4, 27.5. All other spectroscopic data are identical to those reported by Viswanadham *et al.*[39]

Unsymmetrical pyronin dye [2097130–10–2] (AR116). A mixture of 4-(diethylamino)salicylaldehyde (568 mg, 2.94 mmol, 1.7 equiv.), *N*-Boc-3-iodoaniline **11** (552 mg, 1.73 mmol, 1 equiv.), finely ground K_3PO_4 (732 mg, 3.45 mmol, 2 equiv.), CuI (33 mg, 0.17 mmol, 0.1 equiv.) and picolinic acid (43 mg, 0.35 mmol, 0.2 equiv.) in dry DMSO (4.2 mL) was heated in a sealed tube at 90 °C overnight. The reaction was checked for completion by TLC (eluent: DCM 100%, R_f = 0.50) and diluted with EtOAc. Then, the resulting mixture was washed with deionized water thrice and brine, dried over anhydrous Na_2SO_4, filtered and concentrated under reduced pressure. The resulting residue was purified by flash-column chromatography over silica gel (step gradient of EtOAc in heptane from 10% to 20%). The crude mixed bis-aryl ether **12** was directly dissolved in 55 : 45 (v/v) TFA–DCM (1.6 mL). The reaction mixture was stirred at RT for 30 min, and evaporated under reduced pressure. The resulting residue was purified by flash-column chromatography (step gradient of MeOH in DCM from 0% to 10%) to provide pyronin **AR116** as a dark purple powder (65 mg, 0.24 mmol, overall yield for two steps 14%). All spectroscopic data are identical to those recently reported by us.[10]

Conflicts of interest

The authors declare no conflicts of interest.

Acknowledgements

This work is supported by the CNRS, Université de Bourgogne and Conseil Régional de Bourgogne through the "Plan

d'Actions Régional pour l'innovation (PARI)" and the "Fonds Européen de Développement Régional (FEDER)" programs. S. D. gratefully acknowledges the Burgundy region ("FABER" programme, PARI Action 6, SSTIC 6 "Imagerie, instrumentation, chimie et applications biomédicales") for his Ph. D. grant (2014–2017). Financial support from Agence Nationale de la Recherche (ANR, AAPG 2018, PRCI LuminoManufacOligo, ANR-18-CE07–0045–01), especially for the post-doc fellowship of K. R., the National Research Foundation Singapore (NRF, LuminoManufacOligo, NRF2018-NRF-ANR035) and GDR CNRS "Agents d'Imagerie Moléculaire" (AIM) 2037 is also greatly acknowledged.

The authors thank the "Plateforme d'Analyse Chimique et de Synthèse Moléculaire de l'Université de Bourgogne" (PACSMUB, http://www.wpcm.fr) for access to spectroscopy instrumentation. COBRA lab (UMR CNRS 6014) and Iris Biotech company are warmly thanked for the generous gift of some chemical reagents used in this work. The authors also thank Marie-José Penouilh (University of Burgundy, PACSMUB) for HRMS measurements, Dr. Myriam Laly (University of Burgundy, PACSMUB) for the determination of TFA content in samples purified by RP-HPLC, Dr. Ewen Bodio (University of Burgundy, ICMUB, UMR CNRS 6302, OCS team) for access to SAFAS Xenius XC spectrofluorimeter and Drs Valentin Quesneau and Ibai E. Valverde (ICMUB, UMR CNRS 6302) for helpful discussions and relevant comments on this manuscript before publication.

Notes and references

1 (*a*) X. Chen, M. Sun and H. Ma, *Curr. Org. Chem.*, 2006, **10**, 477; (*b*) W. Shi and H. Ma, *Chem. Commun.*, 2011, **48**, 8732; (*c*) J. Chan, S. C. Dodani and C. J. Chang, *Nat. Chem.*, 2012, **4**, 973; (*d*) J. Du, M. Hu, J. Fan and X. Peng, *Chem. Soc. Rev.*, 2012, **41**, 4511; (*e*) J. B. Grimm, L. M. Heckman and L. D. Lavis, *Prog. Mol. Biol. Transl. Sci.*, 2013, **113**, 1; (*f*) Y. Yang, Q. Zhao, W. Feng and F. Li, *Chem. Rev.*, 2013, **113**, 192; (*g*) X. Li, X. Gao, W. Shi and H. Ma, *Chem. Rev.*, 2014, **114**, 590.

2 For selected reviews, see: (*a*) L. D. Lavis and R. T. Raines, *ACS Chem. Biol.*, 2014, **9**, 855; (*b*) H. Chen, B. Dong, Y. Tang and W. Lin, *Acc. Chem. Res.*, 2017, **50**, 1410; (*c*) F. de Moliner, N. Kielland, R. Lavilla and M. Vendrell, *Angew. Chem., Int. Ed.*, 2017, **56**, 3758; (*d*) L. D. Lavis, *Annu. Rev. Biochem.*, 2017, **86**, 825; (*e*) X. Luo, J. Li, J. Zhao, L. Gu, X. Qian and Y. Yang, *Chin. Chem. Lett.*, 2019, **30**, 839.

3 (*a*) J. Zhou and H. Ma, *Chem. Sci.*, 2016, **7**, 6309; (*b*) B. M. Luby, D. M. Charron, C. M. MacLaughlin and G. Zheng, *Adv. Drug Delivery Rev.*, 2017, **113**, 97; (*c*) Y. Fu and N. S. Finney, *RSC Adv.*, 2018, **8**, 29051.

4 (*a*) H. Zheng, X.-Q. Zhan, Q.-N. Bian and X.-J. Zhang, *Chem. Commun.*, 2013, **49**, 429; (*b*) Y. Tang, D. Lee, J. Wang, G. Li, J. Yu, W. Lin and J. Yoon, *Chem. Soc. Rev.*, 2015, **44**, 5003.

5 (*a*) Q. Wu and E. V. Anslyn, *J. Mater. Chem.*, 2005, **15**, 2815; (*b*) E. V. Anslyn, *J. Am. Chem. Soc.*, 2010, **132**, 15833; (*c*) Y. Yang, S. K. Seidlits, M. M. Adams, V. M. Lynch, C. E. Schmidt, E. V. Anslyn and J. B. Shear, *J. Am. Chem. Soc.*, 2010, **132**, 13114.

6 (*a*) A. Romieu, *Org. Biomol. Chem.*, 2015, **13**, 1294; (*b*) T. He, H. He, X. Luo, Y. Yang and Y. Yang, *Sci. Sin.: Chim.*, 2017, **47**, 945.

7 For selected examples, see: (*a*) X. Liu, A. Zheng, D. Luan, X. Wang, F. Kong, L. Tong, K. Xu and B. Tang, *Anal. Chem.*, 2017, **89**, 1787; (*b*) S.-L. Pan, K. Li, L.-L. Li, M.-Y. Li, L. Shi, Y.-H. Liu and X.-Q. Yu, *Chem. Commun.*, 2018, **54**, 4955.

8 (*a*) T.-H. Kim and T. M. Swager, *Angew. Chem., Int. Ed.*, 2003, **42**, 4803; (*b*) W. Jiang and W. Wang, *Chem. Commun.*, 2009, 3913; (*c*) J. H. Do, H. N. Kim, J. Yoon, J. S. Kim and H.-J. Kim, *Org. Lett.*, 2010, **12**, 932; (*d*) T.-I. Kim, M. S. Jeong, S. J. Chung and Y. Kim, *Chem. – Eur. J.*, 2010, **16**, 5297; (*e*) T.-I. Kim, H. Kim, Y. Choi and Y. Kim, *Chem. Commun.*, 2011, **47**, 9825; (*f*) D. Kim, S. Sambasivan, H. Nam, K. Hean Kim, J. Yong Kim, T. Joo, K.-H. Lee, K.-T. Kim and K. Han Ahn, *Chem. Commun.*, 2012, **48**, 6833; (*g*) D. Kim, S. Singha, T. Wang, E. Seo, J. H. Lee, S.-J. Lee, K. H. Kim and K. H. Ahn, *Chem. Commun.*, 2012, **48**, 10243; (*h*) I. Kim, D. Kim, S. Sambasivan and K. H. Ahn, *Asian J. Org. Chem.*, 2012, **1**, 60; (*i*) H. Mohapatra and S. T. Phillips, *Angew. Chem., Int. Ed.*, 2012, **51**, 11145; (*j*) Y. Peng, Y.-M. Dong, M. Dong and Y.-W. Wang, *J. Org. Chem.*, 2012, **77**, 9072; (*k*) J. Park and Y. Kim, *Bioorg. Med. Chem. Lett.*, 2013, **23**, 2332; (*l*) P. Hou, S. Chen, H. Wang, J. Wang, K. Voitchovsky and X. Song, *Chem. Commun.*, 2014, **50**, 320; (*m*) J. Kim, J. Park, H. Lee, Y. Choi and Y. Kim, *Chem. Commun.*, 2014, **50**, 9353; (*n*) C. Wang, S. Yang, M. Yi, C. Liu, Y. Wang, J. Li, Y. Li and R. Yang, *ACS Appl. Mater. Interfaces*, 2014, **6**, 9768; (*o*) J.-T. Yeh, P. Venkatesan and S.-P. Wu, *New J. Chem.*, 2014, **38**, 6198; (*p*) S. Zhang, J. Fan, S. Zhang, J. Wang, X. Wang, J. Du and X. Peng, *Chem. Commun.*, 2014, **50**, 14021; (*q*) J. Zhou, Y. Li, J. Shen, Q. Li, R. Wang, Y. Xu and X. Qian, *RSC Adv.*, 2014, **4**, 51589; (*r*) S. Debieu and A. Romieu, *Org. Biomol. Chem.*, 2015, **13**, 10348; (*s*) Q. Fang, Q. Liu, X. Song and J. Kang, *Luminescence*, 2015, **30**, 1280; (*t*) Y. Han, C. Yang, K. Wu, Y. Chen, B. Zhou and M. Xia, *RSC Adv.*, 2015, **5**, 16723; (*u*) P. K. Mishra, T. Saha and P. Talukdar, *Org. Biomol. Chem.*, 2015, **13**, 7430; (*v*) H. Mohapatra, H. Kim and S. T. Phillips, *J. Am. Chem. Soc.*, 2015, **137**, 12498; (*w*) G. Zhang, Y. Sun, X. He, W. Zhang, M. Tian, R. Feng, R. Zhang, X. Li, L. Guo, X. Yu and S. Zhang, *Anal. Chem.*, 2015, **87**, 12088; (*x*) H. Zhang, Y. Xie, P. Wang, G. Chen, R. Liu, Y.-W. Lam, Y. Hu, Q. Zhu and H. Sun, *Talanta*, 2015, **135**, 149; (*y*) J. Zhang, Y. Li and W. Guo, *Anal. Methods*, 2015, **7**, 4885; (*z*) Y. Chen, B. Chen, D. Luo, Y. Cai, Y. Wei and Y. Han, *Tetrahedron Lett.*, 2016, **57**, 1192; (*aa*) Y. Chen, M. Zhang, Y. Han and J. Wei, *RSC Adv.*, 2016, **6**, 8380; (*ab*) A. K. Das, S. Goswami, C. K. Quah and H.-K. Fun, *RSC Adv.*, 2016, **6**, 18711; (*ac*) Z. Hu, J. Hu, H. Wang, Q. Zhang, M. Zhao, C. Brommesson, Y. Tian, H. Gao, X. Zhang and K. Uvdal, *Anal. Chim. Acta*, 2016, **933**, 189; (*ad*) D. Kim, S.-Y. Na and H.-J. Kim, *Sens. Actuators, B*, 2016, **226**, 227;

(*ae*) X. Liu, F. Qi, Y. Su, W. Chen, L. Yang and X. Song, *J. Mater. Chem. C*, 2016, **4**, 4320; (*af*) X. Liu, D. Yang, W. Chen, L. Yang, F. Qi and X. Song, *Sens. Actuators, B*, 2016, **234**, 27; (*ag*) F. Qi, X. Liu, L. Yang, L. Yang, W. Chen and X. Song, *Tetrahedron*, 2016, **72**, 6909; (*ah*) J. Zhang, Y. Li, J. Zhao and W. Guo, *Sens. Actuators, B*, 2016, **237**, 67; (*ai*) W. Chen, X. Yue, W. Li, Y. Hao, L. Zhang, L. Zhu, J. Sheng and X. Song, *Sens. Actuators, B*, 2017, **245**, 702; (*aj*) B. Huo, M. Du, A. Gong, M. Li, L. Fang, A. Shen, Y. Lai, X. Bai and Y. Yang, *Anal. Methods*, 2018, **10**, 3475; (*ak*) Y. Kim, M. Choi, S. V. Mulay, M. Jang, J. Y. Kim, W.-H. Lee, S. Jon and D. G. Churchill, *Chem. – Eur. J.*, 2018, **24**, 5623; (*al*) X. Liu, L. He, L. Yang, Y. Geng, L. Yang and X. Song, *Sens. Actuators, B*, 2018, **259**, 803; (*am*) L. Xia, F. Hu, J. Huang, N. Li, Y. Gu and P. Wang, *Sens. Actuators, B*, 2018, **268**, 70; (*an*) L. Yang, Y. Su, Z. Sha, Y. Geng, F. Qi and X. Song, *Org. Biomol. Chem.*, 2018, **16**, 1150; (*ao*) J. Hu, T. Liu, H.-W. Gao, S. Lu, K. Uvdal and Z. Hu, *Sens. Actuators, B*, 2018, **269**, 368; (*ap*) L. Yang, Y. Su, Y. Geng, H. Xiong, J. Han, Q. Fang and X. Song, *Org. Biomol. Chem.*, 2018, **16**, 5036; (*aq*) W. Li, S. Zhou, L. Zhang, Z. Yang, H. Chen, W. Chen, J. Qin, X. Shen and S. Zhao, *Sens. Actuators, B*, 2019, **284**, 30; (*ar*) Y. Liu, W. Yan, H. Li, H. Peng, X. Suo, Z. Li, H. Liu, J. Zhang, S. Wang and D. Liu, *Anal. Methods*, 2019, **11**, 421; (*as*) H. Qin, L. Li, K. Li and Y. Xiaoqi, *Chin. Chem. Lett.*, 2019, **30**, 71; (*at*) J. Wang, C. Li, Q. Chen, H. Li, L. Zhou, X. Jiang, M. Shi, P. Zhang, G. Jiang and B. Z. Tang, *Anal. Chem.*, 2019, **91**, 9388; (*au*) L. Yang, Y. Liu, Y. Li, H. Wang, H. Zhang, J. Xu, L. Ji, Q. Wang and G. He, *Tetrahedron*, 2019, **75**, 130538.

9 (*a*) Z. Lei and Y. Yang, *J. Am. Chem. Soc.*, 2014, **136**, 6594; (*b*) L. Song, Z. Lei, B. Zhang, Z. Xu, Z. Li and Y. Yang, *Anal. Methods*, 2014, **6**, 7597.

10 S. Debieu and A. Romieu, *Org. Biomol. Chem.*, 2017, **15**, 2575.

11 Z. Lei, Z. Zeng, X. Qian and Y. Yang, *Chin. Chem. Lett.*, 2017, **28**, 2001.

12 For selected reviews, see: (*a*) C.-H. Tung, *Biopolymers*, 2004, **76**, 391; (*b*) C. R. Drake, D. C. Miller and E. F. Jones, *Curr. Org. Synth.*, 2011, **8**, 498; (*c*) A. Razgulin, N. Ma and J. Rao, *Chem. Soc. Rev.*, 2011, **40**, 4186; (*d*) W. Chyan and R. T. Raines, *ACS Chem. Biol.*, 2018, **13**, 1810; (*e*) H.-W. Liu, L. Chen, C. Xu, Z. Li, H. Zhang, X.-B. Zhang and W. Tan, *Chem. Soc. Rev.*, 2018, **47**, 7140; (*f*) H. Wei, G. Wu, X. Tian and Z. Liu, *Future Med. Chem.*, 2018, **10**, 2729; (*g*) X. Wu, W. Shi, X. Li and H. Ma, *Acc. Chem. Res.*, 2019, **52**, 1892; (*h*) J. Zhang, X. Chai, X.-P. He, H.-J. Kim, J. Yoon and H. Tian, *Chem. Soc. Rev.*, 2019, **48**, 683.

13 (*a*) R. Kumar, W. S. Shin, K. Sunwoo, W. Y. Kim, S. Koo, S. Bhuniya and J. S. Kim, *Chem. Soc. Rev.*, 2015, **44**, 6670; (*b*) M. H. Lee, A. Sharma, M. J. Chang, J. Lee, S. Son, J. L. Sessler, C. Kang and J. S. Kim, *Chem. Soc. Rev.*, 2018, **47**, 28; (*c*) C. Yan, L. Shi, Z. Guo and W. Zhu, *Chin. Chem. Lett.*, 2019, DOI: 10.1016/j.cclet.2019.08.038, in press.

14 S. Debieu and A. Romieu, *Tetrahedron Lett.*, 2018, **59**, 1940.

15 (*a*) J. Mei, N. L. C. Leung, R. T. K. Kwok, J. W. Y. Lam and B. Z. Tang, *Chem. Rev.*, 2015, **115**, 11718; (*b*) H. Yuning, *Methods Appl. Fluoresc.*, 2016, **4**, 022003.

16 H. McNab, *Chem. Soc. Rev.*, 1978, **7**, 345.

17 O. A. Argintaru, 1,3-Dimethylbarbituric Acid, in *e-EROS Encyclopedia of Reagents for Organic Synthesis*, John Wiley & Sons, 2011, DOI: 10.1002/047084289X.rn01256.

18 O. Yonemitsu, K. Elghanian and A. C. Hart, 2,2-Dimethyl-1,3-dioxane-4,6-dione, in *e-EROS Encyclopedia of Reagents for Organic Synthesis*, John Wiley & Sons, 2010, DOI: 10.1002/047084289X.rd327m.pub2.

19 P. M. Nowak, F. Sagan and M. P. Mitoraj, *J. Phys. Chem. B*, 2017, **121**, 4554.

20 T. Watanabe, M. Tahara and S. Todo, *Cardiovasc. Ther.*, 2008, **26**, 101.

21 (*a*) Calculated using Advanced Chemistry Development (ACD/Labs) Software V11.02 (© 1994–2019 ACD/Labs); (*b*) W. Ried and P. Stahlhofen, *Chem. Ber.*, 1957, **90**, 828.

22 S. Bloch and G. Toupance, *J. Chim. Phys. Phys.-Chim. Biol.*, 1975, **72**, 1157.

23 A. Khodairy, *Phosphorus, Sulfur Silicon Relat. Elem.*, 2005, **180**, 1893.

24 (*a*) W. Feng, C. Gao, W. Liu, H. Ren, C. Wang, K. Ge, S. Li, G. Zhou, H. Li, S. Wang, G. Jia, Z. Li and J. Zhang, *Chem. Commun.*, 2016, **52**, 9434; (*b*) W. Liu, H. Liu, X. Peng, G. Zhou, D. Liu, S. Li, J. Zhang and S. Wang, *Bioconjugate Chem.*, 2018, **29**, 3332.

25 X. Huang and C. S. Brazel, *J. Controlled Release*, 2001, **73**, 121.

26 M. Beija, C. A. M. Afonso and J. M. G. Martinho, *Chem. Soc. Rev.*, 2009, **38**, 2410.

27 (*a*) A. Loudet, C. Thivierge and K. Burgess, *Dojin News*, 2011, **137**, 1; (*b*) J. Fan, M. Hu, P. Zhan and X. Peng, *Chem. Soc. Rev.*, 2013, **42**, 29.

28 (*a*) W. Zhang, Z. Ma, L. Du and M. Li, *Analyst*, 2014, **139**, 2641; (*b*) B. Daly, J. Ling and A. P. de Silva, *Chem. Soc. Rev.*, 2015, **44**, 4203.

29 Synthesis and study of photophysical properties of this pyronin–coumarin hybrid are planned in the near future.

30 For selected examples: (*a*) H. Lee, M. Y. Berezin, K. Guo, J. Kao and S. Achilefu, *Org. Lett.*, 2009, **11**, 29; (*b*) L. Yuan, W. Lin, S. Zhao, W. Gao, B. Chen, L. He and S. Zhu, *J. Am. Chem. Soc.*, 2012, **134**, 13510.

31 A. N. Butkevich, M. L. Bossi, G. Lukinavičius and S. W. Hell, *J. Am. Chem. Soc.*, 2019, **141**, 981.

32 B. Halliwell and J. M. C. Gutteridge, Glutathione in metabolism and cellular redox state, in *Free Radicals in Biology & Medicine*, Oxford University Press, 5th edn, 2015, pp. 99–104.

33 (*a*) K. Umezawa, M. Yoshida, M. Kamiya, T. Yamasoba and Y. Urano, *Nat. Chem.*, 2017, **9**, 279; (*b*) K. Renault, P.-Y. Renard and C. Sabot, *Eur. J. Org. Chem.*, 2018, 6494.

34 L. He, B. Dong, Y. Liu and W. Lin, *Chem. Soc. Rev.*, 2016, **45**, 6449.

35 (*a*) L. Yu, S. Wang, K. Huang, Z. Liu, F. Gao and W. Zeng, *Tetrahedron*, 2015, **71**, 4679; (*b*) J. L. Kolanowski, F. Liu and

E. J. New, *Chem. Soc. Rev.*, 2018, **47**, 195; (*c*) Y. Yue, F. Huo, F. Cheng, X. Zhu, T. Mafireyi, R. M. Strongin and C. Yin, *Chem. Soc. Rev.*, 2019, **48**, 4155.

36 V. Gupta and K. S. Carroll, *Chem. Sci.*, 2016, **7**, 400.

37 Y. Li, Y. Sun, J. Li, Q. Su, W. Yuan, Y. Dai, C. Han, Q. Wang, W. Feng and F. Li, *J. Am. Chem. Soc.*, 2015, **137**, 6407.

38 G. R. Fulmer, A. J. M. Miller, N. H. Sherden, H. E. Gottlieb, A. Nudelman, B. M. Stoltz, J. E. Bercaw and K. I. Goldberg, *Organometallics*, 2010, **29**, 2176.

39 B. Viswanadham, A. S. Mahomed, H. B. Friedrich and S. Singh, *Res. Chem. Intermed.*, 2017, **43**, 1355.